

Table IV. Summary of Results

complex ^d	vol, cm ³ mol ⁻¹			dist, pm		
	V_{xst}°	V_s°	ΔV°	Δr^a	$\Delta r(M-L)^b$	$\Delta r(\text{xst})$
Fe(HB(pz) ₃) ₂	337.3	337.6	23.6	12		19.9
Fe((acac) ₂ trien) ⁺	265	264	10.3	6.1	11.4	12.6
Fe((sal) ₂ trien) ⁺	275	272	11.9	6.9	13.1	
Co(terpy) ₂ ²⁺	372	368	10.1	4.8		12 ^c

^a Minimum value calculated from V_s° and ΔV , assuming spherical complexes. ^b Calculated from radius of coordination sphere. ^c Average value of two nitrogen atoms at 21 pm and four at 7 pm. ^d Low-spin isomer.

spectively. From the open nature of the complexes revealed in the crystal structures, it is likely that most of the ligand remains solvated in the same way in the two spin states. The effective solvated radius of the metal-ligand core may be taken as the average metal-ligand distance of 193.9 pm plus the average van der Waals radius of the coordinated atoms of 146.7 pm. With this value of 340.6 pm for the solvated radius of the low-spin isomer in solution, the volume differences correspond to metal-ligand bond length changes of 11.4 and 13.1 pm, respectively. These values are in excellent agreement with the difference of 12.6 pm found in the solid state between low-spin [Fe((sal)₂trien)]Cl₂·2H₂O and high-spin [Fe((acac)₂trien)]PF₆.¹⁴ This suggests that the atoms of the first coordination sphere are solvated and that the solvation of the remainder of the ligand is not significantly altered between the spin states. This interpretation is consistent with previous observations¹⁸ of the solvent dependence of the spin equilibrium. This solvent dependence was ascribed to specific hydrogen bonding between the solvent molecules and the N-H protons of the trien ligand, which is manifest in a correlation between the magnetic moment and the N-H stretching frequency.

For [Co(terpy)₂]²⁺ the partial molal volume of 368 cm³ mol⁻¹ corresponds to a spherical radius of 526.4 pm. From the volume difference between the spin states obtained from the pressure measurements, the difference in spherical radii is calculated to be only 4.8 pm. Again this represents a lower limit to the difference in metal-ligand bond lengths. A comparison among a series of [Co(terpy)₂]²⁺ structures indicates that the spin-state change results in a lengthening of the bond to the central nitrogen

of each ligand by as much as 21 pm, but a lengthening of only 7 pm in the bonds to the two distal nitrogens of each ligand.¹⁹ Thus the expansion is concentrated along one axis of the complex. Comparison of the absolute values of the bond length changes suggests solvation of the ligand in both spin states, consistent with the intermolecular overlap of the ligands observed in the crystal structures.

Conclusions

The principal conclusions are summarized in Table IV. The partial molal volumes found for these relatively large metal complexes in solution are very close to the volumes occupied in crystals of the compounds. Analysis of the volume difference between the high-spin and low-spin isomers of these spin-equilibrium complexes provides information about the solvation of the complexes that is not available from the partial molal volumes alone. The larger complexes display larger volume differences between their low-spin and high-spin isomers, consistent with a larger excluded volume. (Note that the iron complexes undergo a change of two-electrons in the antibonding e_g* orbitals while the cobalt(II) complex undergoes a one-electron change. Hence the volume difference for the cobalt complex is intrinsically smaller.) The changes in metal complex radius between spin states calculated for a spherical complex are much smaller than those observed in crystal structures. This implies that much of the ligand remains solvated to the same extent in both spin states. For the ligands derived from triethylenetetramine in which the coordinated atoms are accessible to hydrogen bonding with the solvent, good agreement is obtained between the calculated and observed metal-ligand bond length changes, assuming solvation of the first coordination sphere of the complex, consistent with previous observations of a correlation between the spin equilibrium and amine-hydrogen stretching frequencies.¹⁸

Acknowledgment. This work was supported by the Australian Research Grants Scheme. We thank Dr. Geoffrey Lawrence, now at the University of Newcastle, for assistance with the spin-pressure spectrophotometry at the University of Melbourne.

Registry No. Fe(HB(pz)₃)₂, 16949-45-4; [Fe((acac)₂trien)]NO₃, 68108-57-6; [Fe((sal)₂trien)]NO₃, 67225-84-7; [Co(terpy)₂]Cl₂, 26096-47-9; tetrahydrofuran, 109-99-9.

(18) Tweedle, M. F.; Wilson, L. J. *J. Am. Chem. Soc.* **1976**, *98*, 4824.

(19) Figgis, B. N.; Kucharski, E. S.; White, A. H. *Aust. J. Chem.* **1983**, *36*, 1537.

Contribution from the Research School of Chemistry, Australian National University, Canberra 2601, Australia, and Division of Applied Organic Chemistry, CSIRO, Melbourne 3001, Australia

Low-Temperature IR MCD Using Modified PTFE Films and Applications to the Creutz-Taube Complex

Elmars R. Krausz*[†] and Albert W. H. Mau[‡]

Received July 18, 1985

We report the use of a PTFE polymer with ion-exchange properties (Nafion), to prepare very thin films containing a high concentration of a cationic species under study. These films are remarkably transparent throughout the near- and mid-IR regions and have the particular advantages (for MCD measurements) of being both optically isotropic and transparent. We present MCD spectra of the Creutz-Taube mixed-valence ion, which exhibit both vibrational and electronic MCD spectral features in the IR region. Spectra of related monomeric materials dispersed in KCl disks are also presented. The presence of an electronic transition near 2000 cm⁻¹ in the Creutz-Taube complex, predicted by a previous theoretical analysis, is confirmed. The reported spectra appear to be the first low-temperature IR MCD spectra in the range from 1800 to 2500 cm⁻¹.

1. Introduction

Spectral transmission measurements made in the IR region are usually made on gases, solutions, mulls, and pressed disks. Single crystals of suitable size and thickness can seldom be prepared.

Furthermore, in crystals, there are problems in accounting for reflectivity dispersions arising from changes in the real part of the dielectric constant. The magnetic circular dichroism (MCD) technique¹ has recently been extended to the IR region,^{2,3} but

[†] Australian National University.
[‡] CSIRO.

(1) Piepho, S. B.; Schatz, P. N. *Group Theory in Spectroscopy, with Applications to Magnetic Circular Dichroism*; Wiley-Interscience: New York, 1983.

measurements have been limited to the measurement on liquids at room temperature, partly because of the difficulty in sealing low-temperature cryostat windows, but also because of the lack of a suitable host medium in which to place a species under study. For MCD measurements, single-crystal measurements place the extra constraint of optical isotropy in at least one direction. Frozen solutions are often unsatisfactory as they can crystallize and depolarize radiation through scattering and strain birefringence. Absorptions in the polar solvents needed for ionic species also severely limit the usable spectral range.

A number of low-temperature measurements in the near-IR region (1–2.5 μm) have been made recently,^{4,5} using poly(vinyl alcohol) (PVA) as a host medium. PVA is opaque at energies less than 4000 cm^{-1} . PVA also has a limited ability to dissolve most ionic species. A comparison of spectra of a number of inorganic complexes obtained in PVA (which are solid solutions) with the same complexes made up as conventional KBr and KCl IR pressed disks have shown that spectra were not always in more than qualitative agreement with the solid-solution (PVA) spectra and sometimes were quite different. The discrepancies are much less significant when absorptions are of lower molar extinction and the material disperses well in the powdered halide. There were also dependences on the specific counterion in the material used in the preparation of the disk.

The near-IR and IR spectra of the mixed-valence Creutz-Taube ion are of particular interest due to theoretical predictions of low-energy electronic levels in the vibrational region.^{6,7} Transitions near 2000 and 3200 cm^{-1} are predicted and should show substantial MCD activity according to the electronic coupling model. The low-temperature MCD technique is particularly well suited to search for these transitions for a number of reasons. MCD measurements would be expected to discriminate between vibrational and electronic levels. Nuclear angular momenta are much smaller than electronic angular momenta. For this reason, and the separation of nuclear and electronic motions specified within the Born-Oppenheimer approximation, only very small vibrational MCD would be expected in the absence of substantial vibronic (electronic-nuclear) coupling. Electronic absorptions are generally broader than vibrational transitions and are often difficult to detect in absorption for this reason. The observation of an MCD C type term¹ (with its characteristic $1/T$ dependence) can establish the presence of an absorption system when weak or featureless absorption bands are lost in base lines in the absorption experiment.

2. Experimental Section

2.1. Polymer Film Preparation. The ability to prepare polymers with poly(tetrafluoroethylene) (PTFE) backbones and anionic (or cationic) side chains has been a strongly developing field.^{8,9} These materials are commercially available¹⁰ are commonly used to prepare chemically modified electrodes.¹¹ More recently it has been possible to dissolve these materials in binary solvents under conditions of high pressure and temperature.¹² These solutions may then be used to cast thin films by evaporation. The films can absorb large quantities of metal complex ions.¹¹

Nafion in its protonic form (Du Pont 117) was dissolved in a water/2-propanol mixture by using the technique of Martin et al.¹² A 4% solution was then used to cover a clean, flat optical window to the thickness where surface tension prevented spillage (~ 0.5 mm). This was

then allowed to evaporate at room temperature till dry (~ 1 h) and the process repeated once or twice to increase the thickness and durability of the film. The film thickness was measured by a depth profiler. For IR MCD studies, films 20 μm thick were found to be suitable.

Removal of the dried film from the glass support was effected by dipping the window slowly into water and using the surface tension of the water to lift the film from the surface of the window. The floating Nafion film was then placed directly into an aqueous solution of the Creutz-Taube ion as the tosylate salt. The film immediately started to develop the purple color of the complex and saturated overnight at approximately 0.6 M (as judged from the absorbance of the 6700- cm^{-1} band and the known ϵ). Each Creutz-Taube pentacation, therefore, occupies two sulfonate sites.

Once all the anion sites have been associated with either the cation under study or an appropriate inert cation, there is a small residual absorption at 3500 cm^{-1} due to water that cannot be removed by simple desiccation.¹² This absorption can be used to monitor the thickness of the film in simple cases.¹³ At our low film thicknesses, it is still possible to measure absorptions that have a molar extinction coefficient (ϵ) as low as 10 $\text{L mol}^{-1} \text{cm}^{-1}$. The counterion used in the solution is irrelevant, as is the degree of solubility of the starting material (in water). These films often extract species from low-concentration solutions to much higher concentrations in the polymer. The counterion is not incorporated into the film to a significant extent.

Deuterated sample films are prepared by immersing the foils in a D_2O solution containing the deuterated sample. The level of deuteration observed in the films is always less than that of the starting material, indicating a significant exchange of deuterons with the protons of the residual water in the film. The level of deuteration of the complex slowly declines over a period of days. A fully deuterated species may require dissolution of the Nafion starting materials in deuterated solvents. We are working toward achieving full deuteration.

The chemical inertness of the polymer allowed (for example) in situ oxidation of the Creutz-Taube ion with bromine vapor. The blank protonic films may be regenerated by soaking them in concentrated nitric acid.

Blank foils showed no observable MCD in the range studied. A careful comparison was made between the MCD of a number species (mixed valence and monomeric), dissolved in PVA and bound to Nafion films. Except for small changes in line widths, spectra were found to be identical, throughout the visible and near-IR regions. We feel that the material can be used with confidence for MCD work. This may not apply to the study of vibrational CD, where the host may have more influence on the species under study and careful checks would need to be made.

2.2. MCD Instrumentation. MCD Spectra were recorded on an apparatus constructed at ANU. We have incorporated a number of significant improvements into the system previously described,⁴ and these have extended the useful range of the instrument to 5.5 μm .

A split-pair 6-T superconducting magnet, encased in a mild steel box, was used. The cryostat had a separate inner cold-tail construction (Oxford Instruments model SM4), allowing routine measurements from 300 down to 1.3 K. However, the standard silica optical windows were not transparent in the IR region. The outer and radiation shield windows were replaced with thick CaF_2 windows. The inner windows however presented more of a problem as they needed to be transparent, strain free, and thermally cyclable to 1.4 K while remaining superfluid helium leak free. One compromise was to construct the inner windows from thin infrared grade silica (Infrasil), which can be reliably sealed, and this allowed measurements down to 4.2 μM . We have been able to construct low-temperature seals to CaF_2 windows in a similar way, and they are reasonably reliable. They must however be treated with care while the magnet system is pumped or cooled.

A 150-W Xenon lamp fitted with a sapphire window (Varian Associates) was used as the light source. The entire apparatus was purged with dry nitrogen. An MgF_2 Rochon polarizer (Karl Lambrecht) was used to polarize the light from the Spex 1704 spectrometer, which was fitted with gratings blazed at 2 and 4 μm . A very simple, inexpensive, and reliable ZnSe photoelastic stress modulator of a new type developed at ANU¹⁴ was used to generate circularly polarized light. A strain-free CaF_2 lens focused light onto the sample, and transmitted light was focused onto a high-quality, small-diameter (1.25 mm) liquid-nitrogen-cooled InSb detector (Cincinnati Associates) by a 6:1 ellipsoidal mirror. All spectra were digitized and corrected for zero-field base lines. With large (3 mm \times 5 mm) samples of optical density less than 0.3, our system is detector light current (shot noise) limited in most of the spectral range.

- (2) Keiderling, T. A. *J. Chem. Phys.* **1981**, *75*, 3639.
- (3) Devine, T. R.; Keiderling, T. A. *J. Phys. Chem.* **1984**, *88*, 390–394.
- (4) Krausz, E. R.; Ludi, A. *Inorg. Chem.* **1985**, *24*, 939–943.
- (5) Dubicki, L.; Ferguson, J.; Krausz, E. R.; Lay, P. A.; Maeder, M.; Magnuson, R. H.; Taube, H. *J. Am. Chem. Soc.* **1985**, *107*, 2167–2171.
- (6) Dubicki, L.; Ferguson, J.; Krausz, E. R. *J. Am. Chem. Soc.* **1985**, *107*, 179–184.
- (7) Piepho, S. B.; Krausz, E. R.; Schatz, P. N. *Chem. Phys. Lett.* **1978**, *55*, 539–542.
- (8) Oyama, N.; Anson, F. C. *J. Electrochem. Soc.* **1980**, *127*, 247.
- (9) Bruce, J. A.; Wrighton, M. S. *J. Am. Chem. Soc.* **1982**, *104*, 72.
- (10) Du Pont Co., Wilmington, DE.
- (11) White, H. S.; Leddy, J.; Bard, A. J. *J. Am. Chem. Soc.* **1982**, *104*, 4811–4817. Buttry, D. A.; Saveant, J. M.; Anson, F. C. *J. Phys. Chem.* **1984**, *88*, 3086–3091.
- (12) Martin, C. R.; Rhoades, T. A.; Ferguson, J. A. *Anal. Chem.* **1982**, *54*, 1639–1641.

(13) Lopez, M.; Kipling, B.; Yaeger, H. L. *Anal. Chem.* **1976**, *48*, 1120–1122.

(14) Ling, W. Patent applied for (1985).

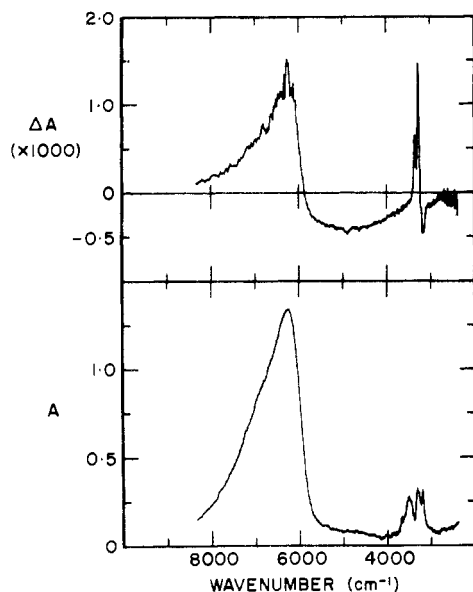


Figure 1. Near-IR MCD (upper) and absorption (lower) of a Nafion film containing the Creutz-Taube ion (~ 0.1 M) at 1.4 K and 3-T field. All features show a $1/T$ dependence between 1.4 and 35 K. Absorption spectra are computer-generated from single-beam transmission spectra of the sample and a hole of the same size.

This apparatus constitutes a significant advance, as it is optimized for IR MCD rather than CD measurements. The small-diameter detector has excellent and uniform radiation sensitivity, and its polarization response (after minimal shielding) is not affected by stray magnetic fields. This allows *precise* subtraction of zero-field signals. Large-diameter detectors are recommended for dispersive vibrational CD work to *reduce* base lines, but this would drastically reduce sensitivity in our apparatus. The development of low-temperature strain-free CaF_2 windows also eliminates a serious technical hurdle.

An immediate extension of our apparatus to 1000 cm^{-1} is being made by replacing the xenon lamp by an intense glow-bar source and the detector by an appropriate HgCdTe IR detector.

3. Absorption and MCD Spectra

The MCD and absorption spectra of a film containing the decaammine(μ -pyrazine- N,N')diruthenium(5+) (Creutz-Taube) ion in the near-IR regions are shown in Figure 1. The higher energy parts of the spectra are in complete accord with the spectra previously published of the same species *dissolved* in PVA.⁴ Excess noise at the peak of the MCD is due to the high optical density of the sample, used to optimize the weaker IR absorption modes. Below the PVA cutoff of 4000 cm^{-1} , the Nafion host spectra show a continuation of the broad negative peak, as well as sharp structure near 3200 cm^{-1} , the C-H and NH_3 stretching frequencies, seen in the absorption spectra.

Figure 2 concentrates on the low-energy region from 1800 to 3000 cm^{-1} , using more concentrated films. Spectra are shown of Nafion films containing the normal and (partially) deuterated Creutz-Taube complex. The residual level of deuteration (section 2.1) is probably over 50%, as the deuteron stretch absorption intensities are considerably less than for the corresponding proton modes. The cause of incomplete deuteration is discussed in section 2.1. Other features are seen in both films at 2000 and 2500 cm^{-1} , as well as a broad negative background. Sharp spikes at 2185, 2100, and 2024 cm^{-1} are not temperature-dependent and are associated with the MCD cryostat system.

Spectra of the normal and partially deuterated tosylate salts of the Creutz-Taube ion, dispersed in KCl disks, are shown in Figure 3. Absorption and MCD spectra of the disks in the near-IR region are only in rough qualitative agreement with the PVA- and Nafion-based spectra. Absorbances in the 1800 – 3500 cm^{-1} region are much lower, leading to less scattering and reduced reflectance anomalies from the microcrystal suspensions (KCl disks), and the spectra are quite similar to the Nafion-based spectra at low energies. The spectra at $<2500\text{ cm}^{-1}$ are almost identical, although the deuterated mode in the KCl disk apparently

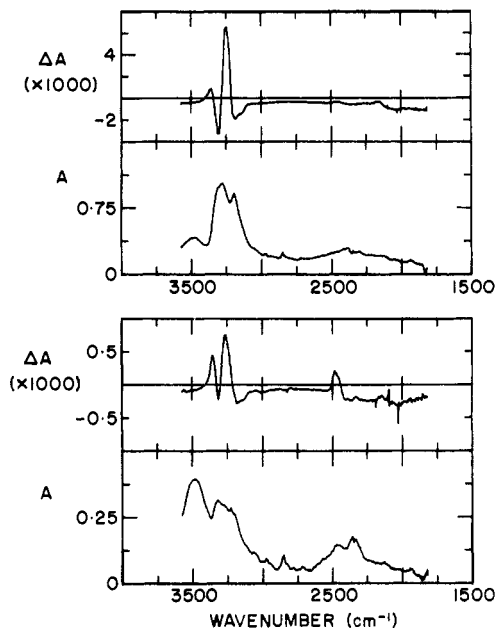


Figure 2. Top: mid-IR MCD and absorption of a Nafion film containing the Creutz-Taube ion (~ 0.3 M). Bottom: corresponding spectra of a partially deuterated film (see text). MCD spectra were recorded at 3 T and 1.37 K.

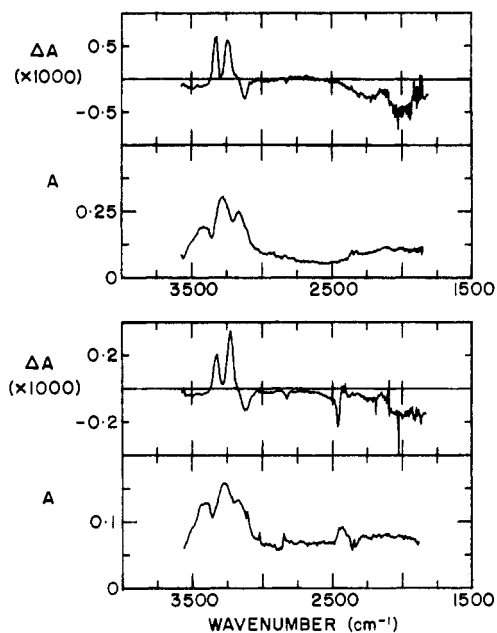


Figure 3. Mid-IR absorption and MCD spectra of the Creutz-Taube tosylate salt, normal (top) and partially ammine deuterated (bottom), dispersed in a KCl disk. Spectra shown were taken at 3 T and 1.37 K and had a $1/T$ dependence in the range 10–30 K.

has the opposite sign in the Nafion host. The MCD of a KCl disk of the chloride salt has a very different MCD spectrum in the 3200 cm^{-1} region but is almost identical in the 1800 – 3000 cm^{-1} region.

Figure 4 shows the absorption and MCD spectra, in the range from 1800 to 4000 cm^{-1} , of $[\text{Ru}(\text{NH}_3)_5(\text{pyrazine})]\text{Tos}_3$ and $[\text{Ru}(\text{ND}_3)_5\text{Cl}]\text{Cl}_2$ monomers carefully dispersed in KCl. The level of deuteration in the chloride is over 95% and unequivocally shows the shift of a sigmoidal vibrational MCD from 3300 to 2400 cm^{-1} upon deuteration. The general shapes and magnitudes of the vibrational MCD from the two systems are similar and each shows a more weakly structured but broad *positive* system in the 2000 cm^{-1} region largely unaffected by deuteration. The residual water absorption at 3500 cm^{-1} shows no MCD signal at the same level of sensitivity.

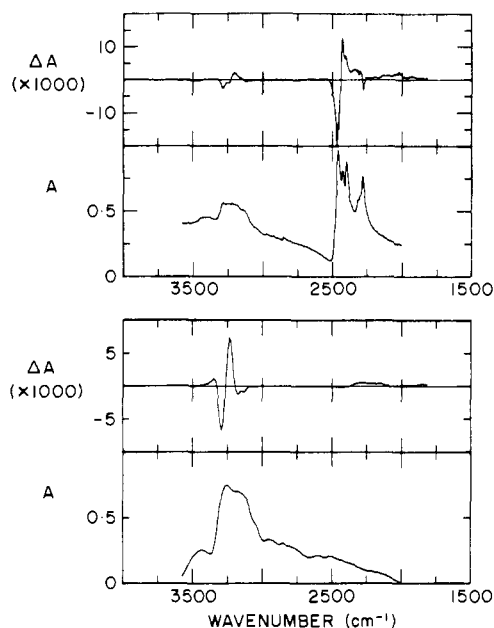


Figure 4. Mid-IR absorption and MCD spectra of the $[\text{Ru}(\text{NH}_3)_5(\text{pyrazine})]\text{Tos}_3$ monomer (top) and $[\text{Ru}(\text{ND}_3)_5\text{Cl}]\text{Cl}_2$ monomer (bottom), dispersed in KCl disks. Spectra shown were taken at 3 T and 1.37 K.

4. Discussion

The sharp features seen near 3200 cm^{-1} in the Creutz-Taube complex do not correspond accurately in position or width to the NH_3 stretching bands that are seen in absorption. All features have been experimentally established as C terms, and the MCD and absorption spectra would be expected to have the same shape for a single electronic level. Attempts to fit the MCD spectral dispersion with a variable combination of the absorption dispersion plus a numerical differential of the absorption dispersion failed completely.

One parity-forbidden and one parity-allowed electronic band have been predicted⁶ to lie at 3201 and 3167 cm^{-1} , respectively.⁶ Deuteration studies in the $3000\text{--}6000\text{ cm}^{-1}$ region¹⁵ show that the sharp features observed are however predominantly vibrational MCD with anomalous intensity. This conclusion is further borne out by observations reported here.

The positive feature seen at 2490 cm^{-1} in Figure 2 is due the ND_3 stretch modes of the partially deuterated complex. It is absent in the original protonated decaammine material. The shape and strength of the vibrational MCD for the deuterated mode are not identical with those of the proton modes, nor are they identical in KCl and Nafion host media. This may be due to the fact that deuterium substitution brings the mode frequencies out of resonance with the electronic absorption regions near 3200 cm^{-1} but more likely is due to the incomplete deuteration of the sample. Figure 4 shows spectra of related monomers, where a completely deuterated sample shows MCD signals very similar to those of the protonated material. Deuterations of *cis* and *trans* ammines in halopentaammines¹⁶ occur at quite different rates. The spectra in Figures 2 and 3 are no doubt biased, due to this selective deuteration effect. The *trans* ammine protons are more acidic and are exchanged more readily.

The strongest vibrational MCD activity is associated with the higher energy component of the (N-H,D) absorption region in both the deuterated and protonated Creutz-Taube materials. In the simple octahedral hexaammine, a small splitting is seen in absorption between bands classified as symmetric and asymmetric stretch frequencies. In the Creutz-Taube dimer there is a substantial difference between the *cis* and *trans* ammines, and the *trans* ammines, which are more influenced by $d\text{-}\pi$ back-bonding, may have absorptions at higher frequencies within the overall bandwidth. It appears that the vibrational MCD is sensitive to

this difference (between *cis* and *trans* ammines). A single sigmoid MCD is seen for the hexaammine, but substituted pentaammines (Figure 4) show some further structure, and a marked double sigmoid is seen in the Creutz-Taube system (Figures 2 and 3).

The MCD associated with purely vibrational motions is expected to be small, as mentioned in the Introduction. Vibrational modes can gain substantial MCD intensity (see ref 18 for a definition of g_{max} or "strength") via vibronic coupling to electronic states ($g_{\text{max}} > 10^{-3}$), but the MCD C type terms associated with electronic transitions will, in general, be orders of magnitude stronger ($g_{\text{max}} > 10^{-1}$).^{17,18} Theoretical studies of C term vibrational MCD have not yet been undertaken and are clearly called for on the basis of our results.

A study of the deuteration effects on the broad MCD between 3200 and 6000 cm^{-1} established¹⁵ this intensity as vibronically induced upon an origin near 3200 cm^{-1} . Except for the new feature at 2400 cm^{-1} attributable to a ND_3 stretch, spectra in the $1800\text{--}3000\text{ cm}^{-1}$ region do not appear to change upon deuteration, in sharp contrast to the $3000\text{--}6000\text{ cm}^{-1}$ region. This is consistent with the intensity being static (allowed) and peaking near 2000 cm^{-1} . The two-center electronic coupling model of Dubicki, Ferguson, and Krausz⁶ (DFK) predicts a statically allowed transition at 1834 cm^{-1} with 29% of the intensity of the near-IR transition at 6170 cm^{-1} . The intensity actually observed, in both absorption and MCD, is much less than predicted, but the full line shape needs to be clarified by measurements at longer wavelengths. The DFK analysis⁶ was based on the assumption of (two) interfering static electric dipole intensity mechanisms. The intensity in the $3200\text{--}6000\text{ cm}^{-1}$ region is $>5\%$ of the intervalence intensity but seems dominantly vibronic. The (static) intensity predicted at 3167 cm^{-1} of 1.8% of the intervalence intensity was not observed, perhaps due to masking by strong vibrational absorptions. Obviously, studies of a completely deuterated sample are indicated.

The vibronic coupling PKS model, also a two-center model, has recently been augmented¹⁹ to include the effects of spin-orbit coupling. These calculations involve a great number of extra parameters but do not provide a convincing analysis (by the authors' own account) of the line shapes they specifically seek to address. Ondrechen and her co-workers²⁰ have stressed the necessity of including the ligand in a direct way in their three-center model. The inclusion of the ligand as an extra center allows the symmetric dimer mode q_+ to become active when intensity profiles are calculated. The PKS model only allows coupling to the antisymmetric q_- mode, by symmetry. We point out that q_+ mode activity would *not* lead to a MCD line shape different from the absorption line shape, as is observed. Only the involvement of non totally symmetric modes (vibronic coupling) can change the overall symmetry of the electronic vibrational state. The Hückel and SCF calculations used in the three-center calculations neglect spin-orbit coupling and therefore cannot account for the low-energy states observed; thus, a synthesis of these two approaches is called for.

One might speculate that the sharp MCD feature at 3200 cm^{-1} is a "tunneling" mode, predicted by PKS calculations,⁷ but this can be dismissed, as similar features are seen in monomers (Figure 4). It also seems unlikely that the tunneling mode would have such a high frequency. Furthermore, tunneling transitions would be expected to have dominantly interior (Z) polarization and be unlikely to give rise to a relatively strong MCD feature.

(17) Pawlikowski, M.; Keiderling, T. A. *J. Chem. Phys.* **1984**, *81*, 4765-4773.

(18) The "strength" of the MCD is considered relative to the absorption process that gives rise to the dichroism. A useful phenomenological estimate is the anisotropy, $g_{\text{max}} = \Delta A_{\text{max}}/A_{\text{max}}$. A_{max} and ΔA_{max} occur at the same frequency for C (and B) terms associated with a single, allowed electronic transition.

(19) Neuschwander, K.; Piepho, S. B.; Schatz, P. N., submitted for publication in *J. Am. Chem. Soc.*

(20) Ondrechen, M. J.; Ellis, D. E.; Ratner, M. A. *Chem. Phys. Lett.* **1984**, *109*, 50-55. Ko, J.; Ondrechen, M. J. *Chem. Phys. Lett.* **1984**, *112*, 507-512. Ondrechen, M. J.; Ko, J.; Root, L. J. *J. Phys. Chem.* **1984**, *88*, 5919-5923.

(15) Krausz, E. *Chem. Phys. Lett.* **1985**, *120*, 113-117.

(16) Krausz, E.; Lay, P. A., unpublished results.

The DFK electronic coupling model does provide a reasonable account of the positions and parities of the IR and near-IR transitions in the Creutz–Taube complex and has some relevance to the MCD spectra. The relative intensities of the transitions do however pose a serious problem and may indicate a limit to the validity of the simple two-center approach in the Creutz–Taube ion. MCD and deuteration studies in the near-IR and IR regions,^{4,15} along with single-crystal polarized studies,⁴ have established substantial non-interior- (*Z*-) polarized and vibronically induced intensity. The vibronically induced (parity-forbidden) intensity problem has not as yet been accessed theoretically for mixed-valence systems. Experimentally, this process is active in a number of mixed-valence systems and seems to involve proton

modes specifically. Ammine stretch and deformation modes couple very strongly to single-ion transitions in Ru(III) monomers.¹⁶ We are currently making further MCD and absorption measurements of a range of strongly coupled mixed-valence dimers, including the osmium analogue of the Creutz–Taube ion, and are recording spectra of analogous monomer materials in Nafion films in order to establish further the generality of these phenomena.

Acknowledgment. E.K. thanks Professor P. N. Schatz for a copy of a manuscript prior to publication¹⁹ and Drs. L. Dubicki and P. Bernhardt for useful discussions.

Registry No. PTFE, 9002-84-0; Creutz–Taube ion, 35599-57-6; Nafion, 39464-59-0.

Contribution from the Laboratoire de Chimie Théorique (UA 506), Université de Paris-Sud, 91405 Orsay Cedex, France, and Department of Chemistry, North Carolina State University, Raleigh, North Carolina 27695-8204

Electronic Structure of Nb₃X₄ Type Compounds

Enric Canadell*† and Myung-Hwan Whangbo*‡

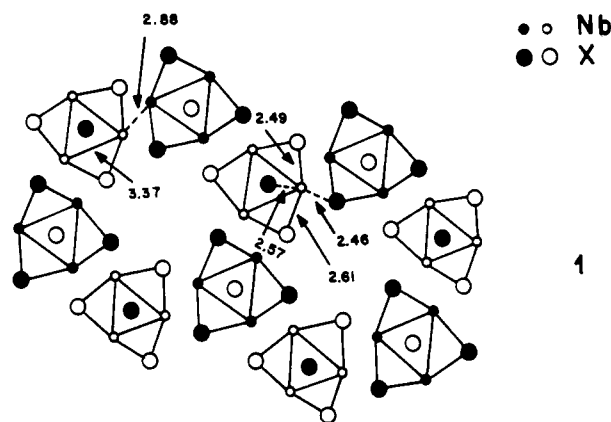
Received October 7, 1985

Tight-binding band calculations were performed on Nb₃S₄ and model Nb₂S₆ chains to examine how the electronic structure of Nb₃S₄ is related to its crystal structure. The low-lying d-block bands of Nb₃S₄ were found to be similar in nature to the t_{2g} subbands of Nb₂S₆ chains of which Nb₃S₄ consists. The low *n*(*e_f*) values of Nb₃X₄ compounds originate from both strong through-space metal–metal 1,2-interactions and good through-bond metal–metal 1,3-interactions within each Nb₂X₆ chain. On the basis of the band electronic structure and the density of states of Nb₃S₄ calculated in the present work, it was found that the Fermi surfaces and the *n*(*e_f*) values of the Nb₃X₄ and Ti₃X₄ lattices can be significantly modified by alkali-metal intercalation.

The crystal structure of triniobium tetrachalcogenides Nb₃X₄ (X = S, Se, Te),¹ discovered more than two decades ago, consists of zigzag Nb chains parallel to the *c* axis. Each zigzag Nb chain is linked to adjacent chains via chalcogen atoms to form hexagonal channels parallel to the *c* axis. Recently, Nb₃X₄ compounds were found to have a number of interesting properties such as superconductivity,² an unusual electrical transport property,^{3a-c} a charge density wave,^{3d} and alkali-metal intercalation.⁴ Available band electronic structure studies on Nb₃X₄⁵ showed that Nb₃X₄ compounds are pseudo one-dimensional metals and that their densities of states at the Fermi level, *n*(*e_f*), are small. These studies were primarily concerned with the electrical transport properties of Nb₃X₄^{5,6} and did not examine how the band electronic structures of Nb₃X₄ are related to their crystal structures. Thus in the present study, the latter question was probed in some detail by performing tight-binding band calculations⁷ on Nb₃S₄ and Nb₂S₆ model chains. The atomic parameters employed in our study are summarized in Table I.

Results and Discussion

A. Crystal Structure. A projected view of Nb₃S₄ along the *c* axis is shown in **1**, where empty and filled circles differ in their heights by *c*/2 along the *c* axis. This diagram, **1**, emphasizes the presence of triangular Nb clusters.^{1,8} Each Nb atom is surrounded by six sulfur atoms that form a distorted octahedron, as can be seen from the Nb–S bond lengths shown in **1**. The triangular Nb clusters are linked via sulfur atoms in such a way that there occur two kinds of sulfur atoms, one surrounded by six Nb atoms and the other surrounded by four Nb atoms. The latter sulfur atoms form hexagonal channels parallel to the *c* axis, which are responsible for alkali-metal intercalation of Nb₃X₄.⁴



As also indicated in **1**, the shortest Nb–Nb distance is 3.37 Å within a triangular Nb cluster but 2.88 Å between adjacent

- (1) (a) Selte, K.; Kjekshus, A. *Acta Crystallogr.* **1964**, *17*, 1568. (b) Ruysink, A. F. J.; Kadijk, F.; Wagner, A. J.; Jellinek, F. *Acta Crystallogr., Sect. B: Struct. Crystallogr. Cryst. Chem.* **1968**, *B24*, 1614.
- (2) Amberger, E.; Polborn, K.; Grimm, P.; Dietrich, M.; Obst, B. *Solid State Commun.* **1978**, *26*, 943.
- (3) (a) Ishihara, Y.; Nakada, I. *Solid State Commun.* **1983**, *45*, 129. (b) Ishihara, Y.; Nakada, I.; Suzuki, K.; Ichihara, M. *Solid State Commun.* **1984**, *50*, 657. (c) Rashid, M. H.; Sellmyer, D. J. *Phys. Rev. B: Condens. Matter* **1984**, *29*, 2359. (d) Suzuki, K.; Ichihara, M.; Nakada, I.; Ishihara, Y. *Solid State Commun.* **1984**, *52*, 743.
- (4) (a) Schöllhorn, R. *Angew. Chem., Int. Ed. Engl.* **1980**, *19*, 983. (b) Schöllhorn, R.; Kuhlmann, R.; Besenhard, J. O. *Mater. Res. Bull.* **1976**, *11*, 83. (c) Schöllhorn, R.; Schramm, W.; Fenske, D. *Angew. Chem., Int. Ed. Engl.* **1980**, *19*, 492. (d) Schöllhorn, R.; Schramm, W. *Z. Naturforsch., B: Anorg. Chem., Org. Chem.* **1979**, *34B*, 697. (e) Boller, H.; Klepp, K. *Mater. Res. Bull.* **1983**, *18*, 437.
- (5) (a) Oshiyama, A. *Solid State Commun.* **1982**, *43*, 607. (b) Oshiyama, A. *J. Phys. Soc. Jpn.* **1983**, *52*, 587. (c) Bulet, D. W. *J. Solid State Chem.* **1980**, *33*, 13.

* Université de Paris-Sud.

† North Carolina State University.